

Expansion history and $f(R)$ modified gravity

Malcolm Fairbairn¹ and Sara Rydbeck³

¹CERN Theory Division, CH-1211, Geneva 23, Switzerland

³Department of Physics, Stockholm University,
Albanova University Center, S-106 91 Stockholm, Sweden

Abstract. We attempt to fit cosmological data using $f(R)$ modified Lagrangians containing inverse powers of the Ricci scalar varied with respect to the metric. While we can confirm the $a \propto t^{1/2}$ behaviour at medium to high redshifts reported elsewhere, we are still able to fit the supernova, CMB and baryon oscillation data. The age of the universe is also compatible with globular clusters. We show, however, that this class of models can be ruled out by considering the thickness of the last scattering surface.

E-mail: `malc@cern.ch, sararyd@physto.se`

1. Introduction

Observations of type 1a supernovae still consistently suggest that the universe is accelerating [1, 2, 3] (see [4] for a detailed list of references). This conclusion seems to be supported by the fact that observations of the CMB tell us that the universe is spatially flat [5] and that the matter which is observed in the universe from galaxy clustering is not enough to account for this flatness [6, 7]. Furthermore, the measurement of space-time geometry achieved by the detection of the imprint of the waves in the primordial plasma in the galaxy correlation function [8] has caused problems for models where the supernova data are explained by the dimming of photons [9, 10, 11].

There have been a number of different approaches trying to explain the mystery of the acceleration of the universe. One such approach consists of a class of theories obtained when the Einstein-Hilbert Lagrangian is modified by hand and the Ricci scalar R is replaced with some function $f(R)$ [12, 13]. These theories are phenomenological in as much as it is not clear what the underlying theory that gives rise to them would be. The motivation is that inverse powers of the curvature in the Lagrangian will give vacuum solutions which are not Minkowski leading to late time acceleration. The simplest theory with inverse powers of the curvature in the Lagrangian is

$$S = \frac{M_{Pl}^2}{2} \int d^4x \sqrt{-g} \left(R - \frac{\mu^4}{R} \right) + \int d^4x \sqrt{-g} \mathcal{L}_M \quad (1)$$

where μ is a mass scale that must be fitted to the data. Variation of this action with respect to the metric gives new field equations

$$\left(1 + \frac{\mu^4}{R^2} \right) R_{\mu\nu} - \frac{1}{2} \left(1 - \frac{\mu^4}{R^2} \right) R g_{\mu\nu} + \mu^4 [g_{\mu\nu} \nabla_\alpha \nabla^\alpha - \nabla_\mu \nabla_\nu] R^{-2} = \frac{T_{\mu\nu}^M}{M_{Pl}^2} \quad (2)$$

from which it can be seen that for cosmological solutions there will exist a vacuum solution with $H \sim \mu$. Such $f(R)$ models can therefore give rise to late time acceleration which could be responsible for the apparent dark energy.

The simplest models of this nature seem to be at odds with solar system tests of gravity, at best containing a light degree of freedom [14] and at worst possessing instabilities [15, 16] but one might imagine that the Lagrangian (1) is some effective limit valid on very large scales and that some new physics on short distances could change the theory. There are also indications that the theories may be safe in some regions of parameter space [17] through a process rather similar to the chameleon mechanism [18].

It should be noted that variation of the normal Einstein-Hilbert Lagrangian with respect to the metric or alternatively the Christoffel symbols leads to the same field equations for gravity whereas in this class of modified Lagrangians the same is not true. Field equations obtained using the latter Palatini approach will yield different cosmologies and solar system constraints [19, 20, 21]. In this work we will restrict ourselves to equations of motion obtained by varying the Lagrangian with respect to the metric.

The solution of the field equations for a cosmological background lead to cosmological equations with higher derivative terms, for example for the field equations (2) the tt Friedman equation for a spatially flat universe becomes

$$3H^2 - \frac{\mu^4}{12(\dot{H} + 2H^2)^3} \left(2H\ddot{H} + 15H^2\dot{H} + 2\dot{H}^2 + 6H^4 \right) = \frac{\rho_M}{M_{Pl}^2} \quad (3)$$

which means that there are more degrees of freedom in the space of solutions than solutions of Einstein gravity with a cosmological constant or the standard DGP model. This space of solutions needs to be compared with the data.

If type 1a supernovae are good examples of standard candles as is thought, they can in principle trace out the Hubble diagram in an unambiguous fashion. There is, however, a need for some caution as there are presently ambiguities in the way that one can analyse the data [22, 23] and also in which supernovae should be included in samples to be used for cosmology [1, 2, 3]. In certain situations, these ambiguities are leading to different predictions with regards to which dark energy models are favoured over others [24, 25, 4].

Despite this, all of the supernova surveys seem to agree on some basic facts, namely that the universe is accelerating and that Λ CDM, i.e. a universe composed of matter, radiation and a constant energy density which does not change over time, fits the data rather well, and better than many alternatives motivated by specific physical models.

Expanding the surveyed redshift range is of great importance to investigate the nature of dark energy and to find out in particular whether it is a cosmological constant or not. Thus, the recent compilation of supernova data in [2], including 23 SNIa at $z \geq 1$ from an HST/ACS is a very interesting data set for model comparisons. Riess et al have included data from various sources and re-fitted the light-curves with the MLCS2k2 technique.

We have used the gold set of 182 SNe Ia from Riess et al [2], taking into account the additional redshift error discussed there in the case of the high redshift supernovae for which the redshifts were determined from broad features in the spectra.

Furthermore we have added to this data set the position of the acoustic peak in the SDSS galaxy survey [8] and also the CMB shift parameter [26]. We direct the reader to [4] for more details and discussion on measuring the expansion history with these data sets.

2. Obtaining solutions for $f(R)$ theories.

There are a large number of different $f(R)$ theories with inverse powers of R that one might consider but we will look at the two simplest models that can be written down, namely $f(R) = R - \mu^4/R$ and $f(R) = R - \mu^6/R^2$.

In order to test the $f(R)$ theories, we need $H(z)$, the Hubble expansion rate as a function of redshift. This is rather difficult to obtain from higher order Friedman equations such as (3). We choose to perform a conformal transformation which allows us to treat the problem as one of a scalar field σ with a potential $V(\sigma)$ evolving in an FRW universe where the matter is endowed with a non-standard gravitational coupling set by σ .

Having found the solutions in the Einstein frame for the scale factor, Hubble parameter and the scalar field, we will transform back to the matter frame \ddagger where we will integrate $H(z)$ and compare it with the data.

For an action of the form $f(R)$ with $\partial f/\partial R > 0$, we can perform a conformal transformation to the Einstein frame [27]. The conformal transformation is written

$$\tilde{g}_{\mu\nu} = pg_{\mu\nu}, \quad \frac{\partial f}{\partial R} \equiv p \equiv \exp\left(\sqrt{2/3}\sigma\right) \quad (4)$$

we will continue to use both p and σ even in the same equations to keep expressions compact despite the fact that they can be used interchangeably. The equations can now be written in the more familiar form

$$\tilde{R}_{\mu\nu} - \frac{1}{2}\tilde{R}\tilde{g}_{\mu\nu} = (\nabla_\mu\sigma)\nabla_\nu\sigma - \frac{1}{2}\tilde{g}_{\mu\nu}\tilde{g}^{\alpha\beta}(\nabla_\alpha\sigma)\nabla_\beta\sigma - V(\sigma)\tilde{g}_{\mu\nu} + \frac{\tilde{T}_{\mu\nu}}{M_{Pl}^2} \quad (5)$$

where the potential and the energy-momentum tensor in the Einstein frame are given by [27]

$$V \equiv \frac{(\text{sign})}{2|\partial f/\partial R|} \left(R \frac{\partial f}{\partial R} - f \right) \quad (6)$$

$$\tilde{T}_{\mu\nu} \equiv \frac{T_{\mu\nu}}{p} \quad (7)$$

with $(\text{sign}) = \frac{\partial f}{\partial R}/|\frac{\partial f}{\partial R}|$. The potential V has mass dimension 2 because we have chosen to work with a dimensionless scalar. We denote quantities in the Einstein frame with a

\ddagger the frame where the matter is not coupled to gravity via σ , sometimes called the Jordan frame or more recently the string frame

tilde, for example the time coordinate in the conformal frame Robertson-Walker metric is $d\tilde{t} = \sqrt{p}dt$ and the scale factor $\tilde{a}(t) = \sqrt{p}a(t)$. The equations which need to be solved simultaneously are the equation of motion for σ and the Friedman equation. The latter comes from the time-time component of the transformed Einstein equations

$$3\tilde{H}^2 = \frac{1}{2}\sigma'^2 + V(\sigma) + \frac{\tilde{\rho}_M}{M_{Pl}^2} \quad (8)$$

where a prime denotes differentiation with respect to \tilde{t} , the density $\tilde{\rho}_M = \rho_M/p^2$ and $\tilde{H} = \tilde{a}'/\tilde{a}$. The equation of motion can be obtained from the time component of the divergence or from the covariant derivative of the stress energy tensor \tilde{T}

$$\sigma'' + 3\tilde{H}\sigma' + \frac{\partial V}{\partial \sigma} - \frac{(1-3w)}{\sqrt{6}}\frac{\tilde{\rho}_M}{M_{Pl}^2} = 0 \quad (9)$$

Equations (8) and (9) are the ones that we need to solve to get the evolution of the universe in these models. In order to relate the Hubble parameter H in the matter frame and \tilde{H} in the conformal frame, one must use

$$H = \sqrt{p} \left(\tilde{H} - \frac{\sigma'}{\sqrt{6}} \right). \quad (10)$$

To compare these models with the data, we need $H(z)/H_0$ in the matter frame, or rather $\int \frac{dz}{H(z)/H_0}$. There are more free parameters than Λ CDM so we restrict ourselves to the case $k = 0$. For a flat universe, our free parameters are Ω_M as defined in the original matter frame, the mass scale μ and the values today of σ and σ' . To write these in dimensionless form, let us introduce the time-variable $\tau = \tilde{H}_0\tilde{t}$ and the parameters

$$\alpha = \frac{H_0}{\mu} \quad \beta = 1 - \frac{1}{\sqrt{6}} \frac{\partial \sigma}{\partial \tau} \Big|_0 \quad (11)$$

where the subscript 0 denotes the values today at redshift $z = 0$. If we also introduce the dimensionless potential $U(\sigma)$ so that

$$V(\sigma) = \mu^2 U(\sigma) \quad (12)$$

then the $\tau\tau$ Friedman equation becomes

$$\frac{\tilde{H}^2}{\tilde{H}_0^2} = \frac{1}{6} \left(\frac{\partial \sigma}{\partial \tau} \right)^2 + \frac{1}{3} \frac{p_0 \beta^2}{\alpha^2} U(p) + \frac{\Omega_M \beta^2}{\sqrt{p_0 p}} \left(\frac{\tilde{a}_0}{\tilde{a}} \right)^3 \quad (13)$$

while the equation of the motion for the scalar field is written

$$\frac{\partial^2 \sigma}{\partial \tau^2} + 3 \frac{\tilde{H}}{\tilde{H}_0} \frac{\partial \sigma}{\partial \tau} + \frac{p_0 \beta^2}{\alpha^2} \frac{\partial U}{\partial \sigma} - \sqrt{\frac{3}{2}} \frac{\Omega_M \beta^2}{\sqrt{p_0 p}} \left(\frac{\tilde{a}_0}{\tilde{a}} \right)^3 = 0. \quad (14)$$

By solving (13) and (14) numerically, we can recover the evolution of the Hubble expansion in the Einstein frame and can convert this back to the matter frame using $\sigma(\tau)$. One of the parameters can be written in terms of the others using (13) with $z = 0$

$$\alpha^2 = \frac{p_0^2 \beta U(p_0)}{3(2p_0 - p_0 \beta - \Omega_M \beta)} \quad (15)$$

We therefore choose to label the parameter space of solutions of $H(z)/H_0$ with the three variables Ω_M , σ_0 and $d\sigma/d\tau|_0$.

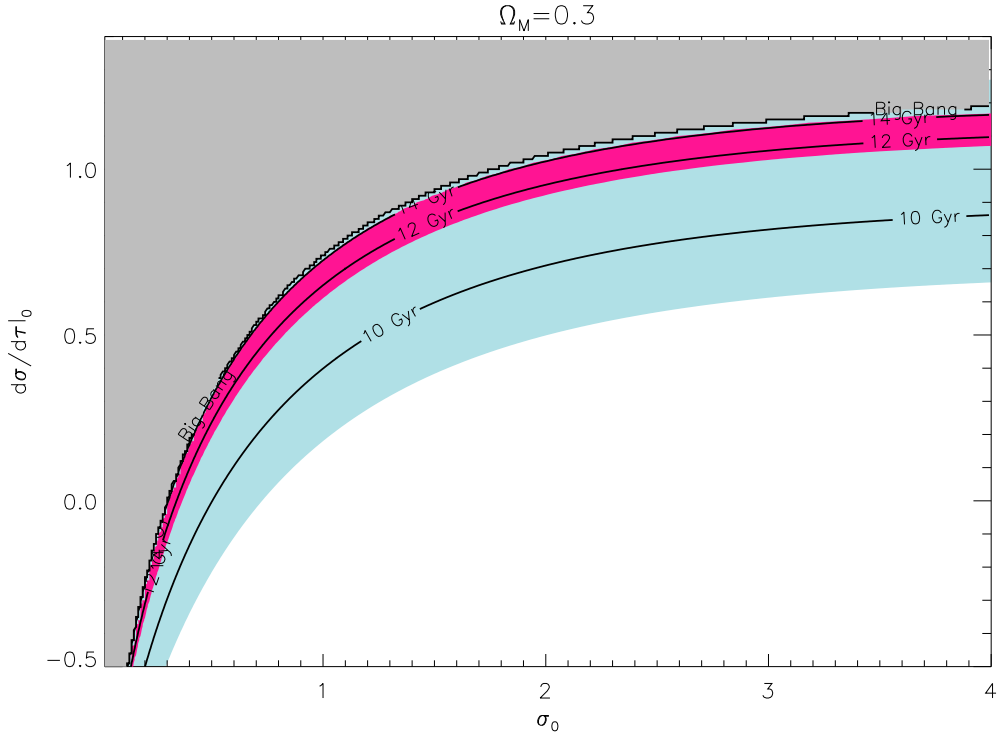


Figure 1. Look back times (age of the universe) for $f(R) = R - \mu^4/R$ cosmologies. We label different cosmologies using the value of the effective scalar σ and its time derivative in the Einstein frame $d\sigma/d\tau$ at redshift $z = 0$. These two parameters plus the matter density (this plot is for $\Omega_M = 0.3$) provide three of the four parameters necessary to determine the cosmology. The fourth is the Hubble constant which is integrated over in cosmological fits. Look-back times are in years in the matter frame assuming a Hubble constant of $65 \text{ km s}^{-1} \text{ Mpc}^{-1}$. In cosmologies above the line labeled 'big bang', the scalar field goes over the top of the potential too quickly (see text). The red region is the 99% region fitting to supernova data, the blue region is the same for BAO.

3. The data vs. $f(R) = R - \mu^4/R$ and $f(R) = R - \mu^6/R^2$

The potential $U(\sigma)$ for the $f(R) = R - \mu^4/R$ model is plotted in the first diagram of figure 4, it rises from zero to a maximum and then falls back to zero as σ goes to infinity.

Figure 1 shows the combined best fit regions for the supernova, BAO and CMB data for $\Omega_M = 0.3$ plotted as a function of σ_0 and $d\sigma/d\tau|_0$. Plotted also are look back times for the age of the universe in this model assuming a Hubble constant $H_0 = 65 \text{ km s}^{-1} \text{ Mpc}^{-1}$ (or more precisely the elapsed time in the matter frame since a redshift of $z = 20$) and a line labeled "big bang" which divides the parameter space between the grey region of solutions where the scalar field $\sigma \rightarrow 0$ too quickly in the past, which corresponds to a curvature singularity.

This can be understood in the following way, for a given value of σ_0 , increasing values of $d\sigma/d\tau$ push σ higher up the effective potential as one moves into the past,

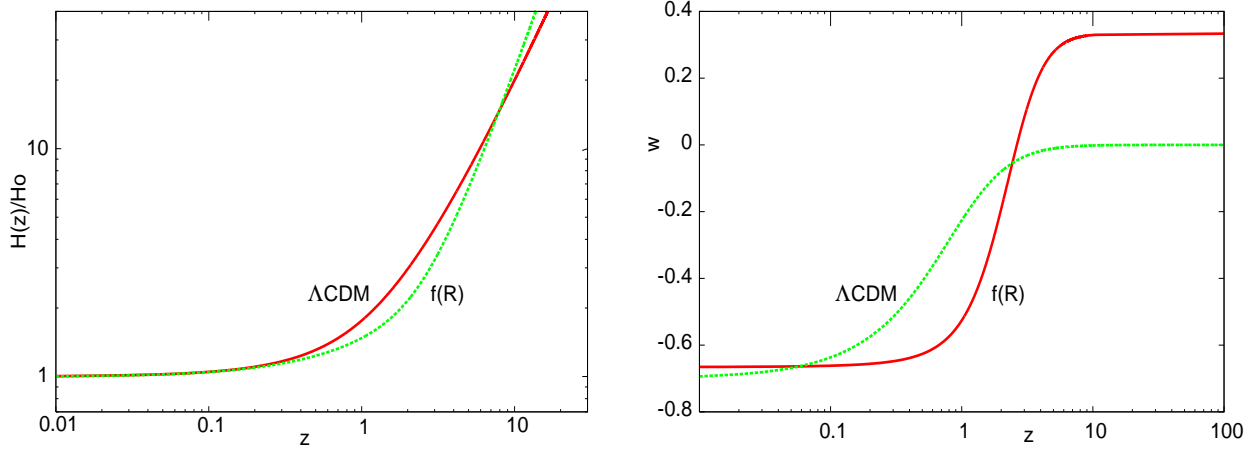


Figure 2. Comparison of the best fit version of $f(R) = R - \mu^4/R$ vs. Λ CDM, in both cases $\Omega_M = 0.3$. On the left $H(z)/H_0$ and on the right the total effective equation of state w defined in equation (16).

which means that the rapidly redshifting contribution from Ω_M can be reduced and the universe expands more slowly in the past, making it older. This increase in age with $d\sigma/d\tau|_0$ ends abruptly for some value of $d\sigma/d\tau|_0$ where σ goes over the top of the potential and falls to $\sigma = 0$ relatively recently in cosmological terms, which signals that $R \rightarrow \infty$ in the matter frame. That region beyond the curve labeled with the words “big-bang” is therefore not included in the analysis and χ^2 values are not calculated there.

Also plotted are the 99% confidence bands for the supernova data in red and the baryon oscillation data in blue. These regions overlap each other for certain values of Ω_M and therefore seem compatible with the model.

The best fit χ^2 values are all rather close to the dividing line to the region where these maximum age cosmologies exist. In these models, the scalar field runs back from the top of the potential so that $\sigma \rightarrow \infty$, $R \rightarrow 0$ and the effective total equation of state $w \rightarrow 1/3$. Speaking purely in terms of expansion history, the universe therefore becomes effectively radiation dominated very recently as we go back in time, not because of the energy density of any radiation, but simply because of the modified gravity giving rise to what looks like, from the FRW perspective, an energy density with equation of state $w = 1/3$. This has been noticed by other authors [28, 29].

On the right of figure 2 is plotted the effective total equation of state that one would obtain if the same expansion was due to some energy density rather than a different theory of gravity, in other words

$$w = \frac{2}{3} \frac{(1+z)}{H} \frac{dH}{dz} - 1 \quad (16)$$

and it can be seen that at high redshifts, $w \rightarrow 1/3$ which is the same as pure radiation.

On the left of figure 2 we can see that $H(z)/H_0$ is similar in both cases at low redshifts where the supernova and baryon oscillation data is fitted, then the $H(z)$ for

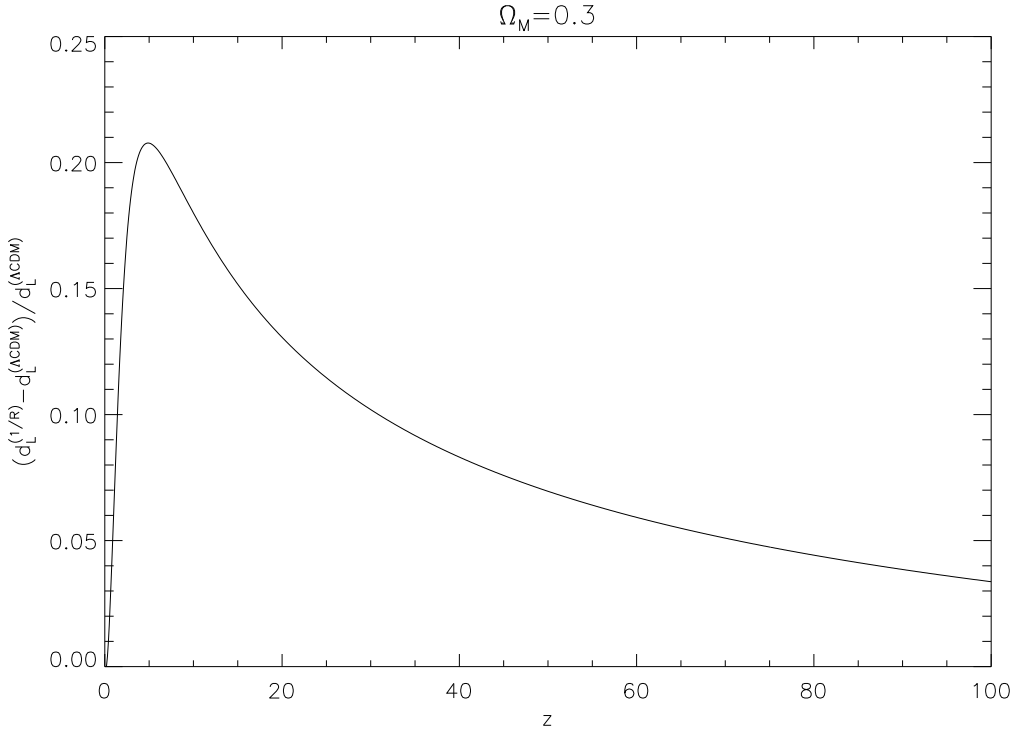


Figure 3. Difference between the luminosity distance as a function of redshift for flat Λ CDM and the best fit $1/R$ model when Ω_M is taken to be 0.3.

the $f(R)$ model dips below, then rises above, the $H(z)$ for Λ CDM. This means that the luminosity/angular distance integrals in both cases can fit the CMB. This point is made clearer by looking at figure 3 which shows the fractional difference between the luminosity distance \S for the $f(R)$ model and the Λ CDM model. The difference between the two is rather small at very low and high redshifts but peaks around $z \sim 5$.

Better knowledge of the Hubble diagram around redshifts of $z \sim 1 - 5$ would therefore probably differentiate between the models, but since we only have good data at $z < 1.5$ from supernovae and at $z \sim 1100$ from the CMB we are not able to differentiate between them using only these data sets.

Figure 4 shows the comparison of the data with the $f(R) = R - \mu^4/R$ model for different values of Ω_M , σ_0 and $d\sigma/d\tau|_0$. Plotted are the banded constraints corresponding to the supernova data and to the baryon oscillation data. A large region of the parameter space is ruled out as it corresponds to regions where $\sigma \rightarrow 0$ too quickly in the past, corresponding to a curvature singularity which would be too recent to accommodate the early universe physics that we know must take place (last scattering surface, nucleosynthesis etc.). The best fit values of χ^2 for different values of Ω_M are listed in table 1 and they show that the model works well in fitting the supernova and the baryon oscillation data. Addition of the CMB data makes the fit worse but it is still

\S and therefore also the angular distance since they are related by a factor of $1+z$

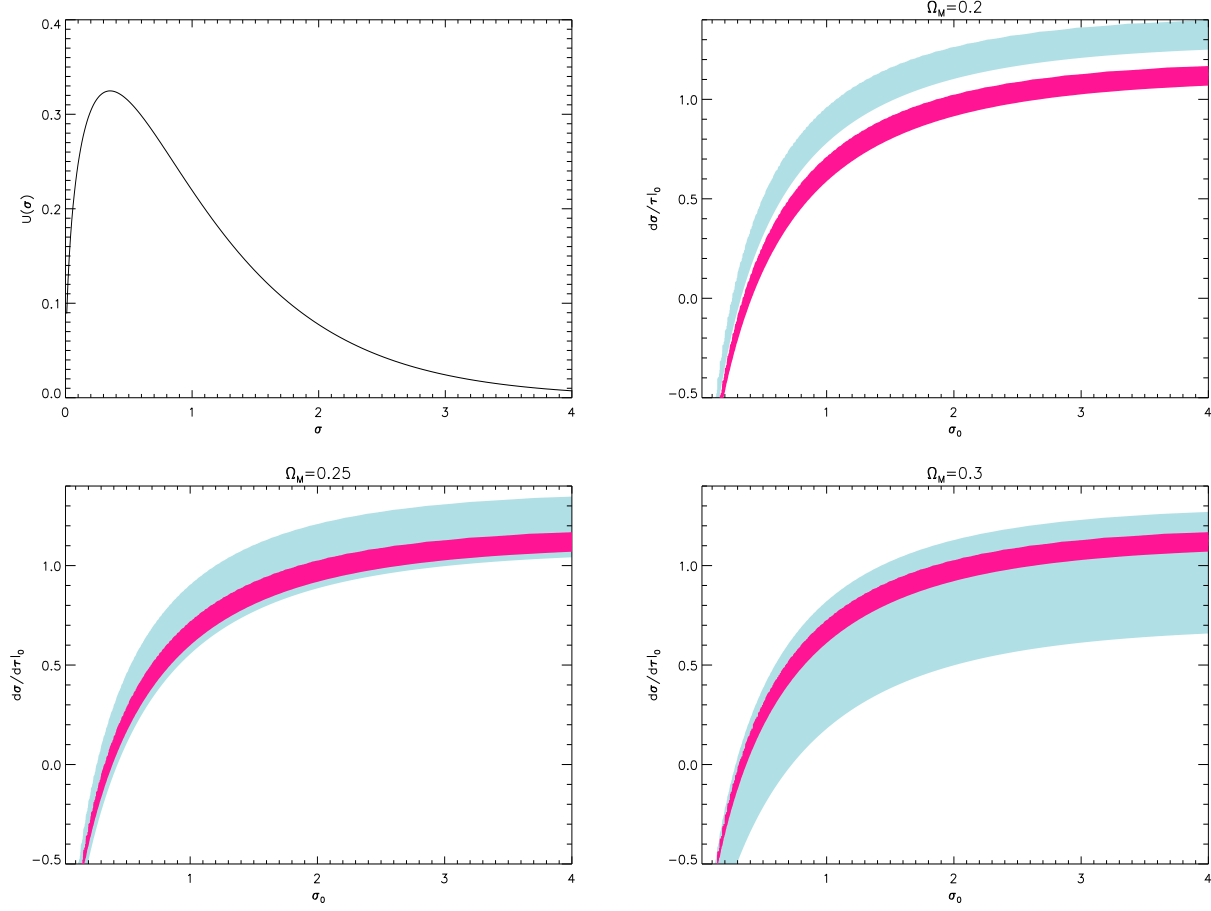


Figure 4. Comparison of $f(R) = R - \mu^4/R$ with data. The top left hand panel is the effective potential in the Einstein frame, while the other three plots are the values of σ_0 and $d\sigma/d\tau|_0$ favoured by the supernova data in red and the BAO data in blue (see caption of figure 1 for more details explaining the plot). The three plots correspond to different matter densities - $\Omega_M = 0.2, 0.25, 0.3$.

$\Omega_M =$	$R - \mu^4/R$			$R - \mu^6/R^2$		
	0.2	0.25	0.3	0.2	0.25	0.3
χ^2_{min} (SNe+flat)	155	155	155	156	156	156
χ^2_{min} (SNe+CMB+flat)	185	180	177	173	163	158
χ^2_{min} (SNe+BAO+flat)	169	156	156	175	159	156
χ^2_{min} (SNe+BAO+CMB+flat)	201	182	179	186	164	159

Table 1. The best fit values of χ^2 for the $-\mu^4/R$ and the $-\mu^6/R^2$ modifications of the Einstein-Hilbert Lagrangian. The vertical columns correspond to different values of Ω_M while each row corresponds to a different subset of the data. Flatness is assumed throughout.

possible to fit the data with a χ^2 per degree of freedom which is less than one. Also the look back time is consistent with the age of globular clusters [30].

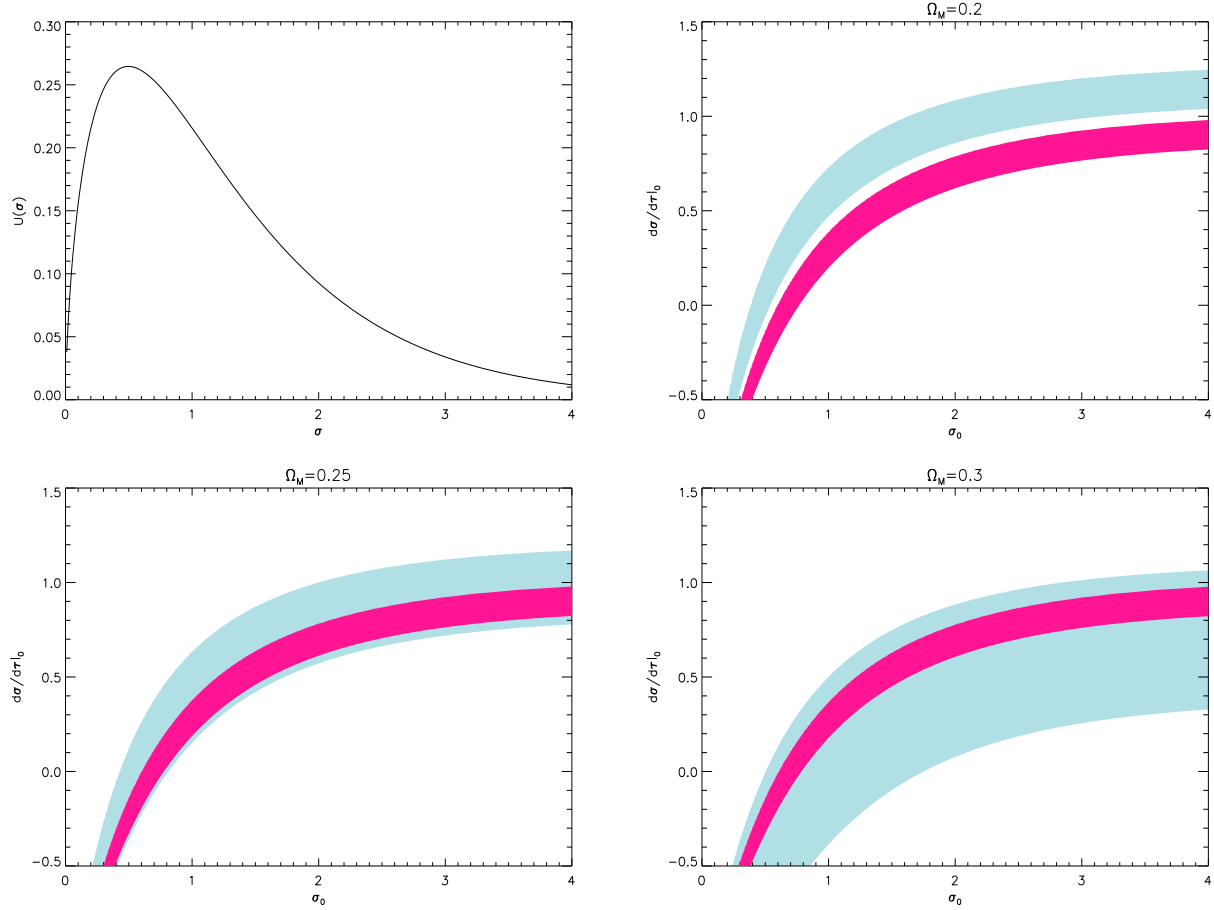


Figure 5. Comparison of $f(R) = R - \mu^6/R^2$ with data. The top left hand panel is the effective potential in the Einstein frame, while the other three plots are the values of σ_0 and $d\sigma/d\tau|_0$ favoured by the supernova data in red and the BAO data in blue (see caption of figure 1 for more details explaining the plot). The three plots correspond to different matter densities - $\Omega_M = 0.2, 0.25, 0.3$.

The same analysis has been carried out for the $f(R) = R - \mu^6/R^2$ model of gravity and the results are listed in figure 5 and the best fit values of χ^2 are listed in table 1. The situation is completely analogous to the $-\mu^4/R$ modifications. Again, the models are able to explain the supernova data and the CMB data simultaneously.

To summarize this section, universes which fit the data in the $1/R$ model lead to the scale factor $a \propto t^{1/2}$ at high redshift. Despite this, the universes obtained are old enough to accommodate globular clusters. Also, because the integrals over $1/H(z)$ are dominated at low redshifts, it is possible to fit the supernova, baryon oscillation and CMB data.

4. Thickness of the Last Scattering Surface.

So far it has been shown that in models of the modified gravity of the form $1/R$ and $1/R^2$, the expansion of the universe from redshift around $z \sim 10$ and onwards is effectively

like that of a radiation dominated universe. Despite this, it can also be shown that the same cosmology can fit the supernova data, the angular size of the observed baryon oscillations and also the angular size of the peak in the CMB. This is not contradictory because at low redshift the $f(R)$ universe is not behaving like a radiation dominated universe, while the relevant integral for the angular position of the peak of the CMB is dominated by the low redshift contribution.

Also the age of the universe is perfectly compatible with the age of globular clusters observed. One therefore cannot use these standard benchmark tests to rule out the model, even though it does not have a prolonged period of radiation domination.

There are of course still unused weapons in our arsenal of observations, in particular one can think about how the perturbations grow in these models, as has been analysed previously in reference [31]. Also one can consider what happens to nucleosynthesis which is in principle rather sensitive to the expansion of the universe during the freeze out of the weak interactions. However, it is simpler and easier to consider the epoch of recombination and to look at the way that the added expansion at redshifts of order $z \sim 1000$ will affect the thickness of the CMB.

The recombination of protons and electrons which occurs as the universe cools is the process responsible for making the universe transparent. In normal cosmologies where the universe is still matter dominated at this epoch, the electrons, photons and protons remain rather close to thermal equilibrium throughout the process. The physics is therefore less dependent upon the expansion rate of the universe but more upon the temperature. However, the effective radiation density that one obtains at high redshifts in the $f(R)$ models considered here is approximately 2 orders of magnitude larger than the energy density of radiation implied from the temperature of the CMB.

The density of radiation implied by looking at the $2.7K$ background radiation is of the order of $\Omega_\gamma \sim 10^{-4}$ so that matter radiation equality occurs at redshifts around a few times 10^4 . The effective radiation density that fits the $H(z)$ at high redshift correspondent to the best fit $1/R$ model (plotted in the left hand panel of Figure 2) is $\Omega_{w=1/3} \sim 0.034$. The expansion rate around $z \sim 1000$ is therefore changed considerably, and recombination takes longer to occur.

The equation which needs to be solved in order to calculate the rate of reionisation is [32, 33]

$$\frac{dx_e}{dz} = \frac{1}{H(1+z)} \left[\alpha n_p x_e^2 - \beta(1-x_e) \exp\left(-\frac{B_1 - B_2}{kT}\right) \right] C \quad (17)$$

where α is the recombination coefficient, β is the ionization coefficient and B_n is the binding energy of the n -th level of the hydrogen atom. The factor C is given by

$$C = \frac{1 + K\Gamma(1 - x_e)}{1 + K(\Gamma + \beta)(1 - x_e)} \quad (18)$$

where Γ is the decay rate of the 2s excited state to the ground state via the emission of 2 photons. The ionisation coefficient β is given by

$$\beta = \alpha \left(\frac{2\pi m_e kT}{h^2} \right)^{3/2} \exp\left(-\frac{B_2}{kT}\right) \quad (19)$$

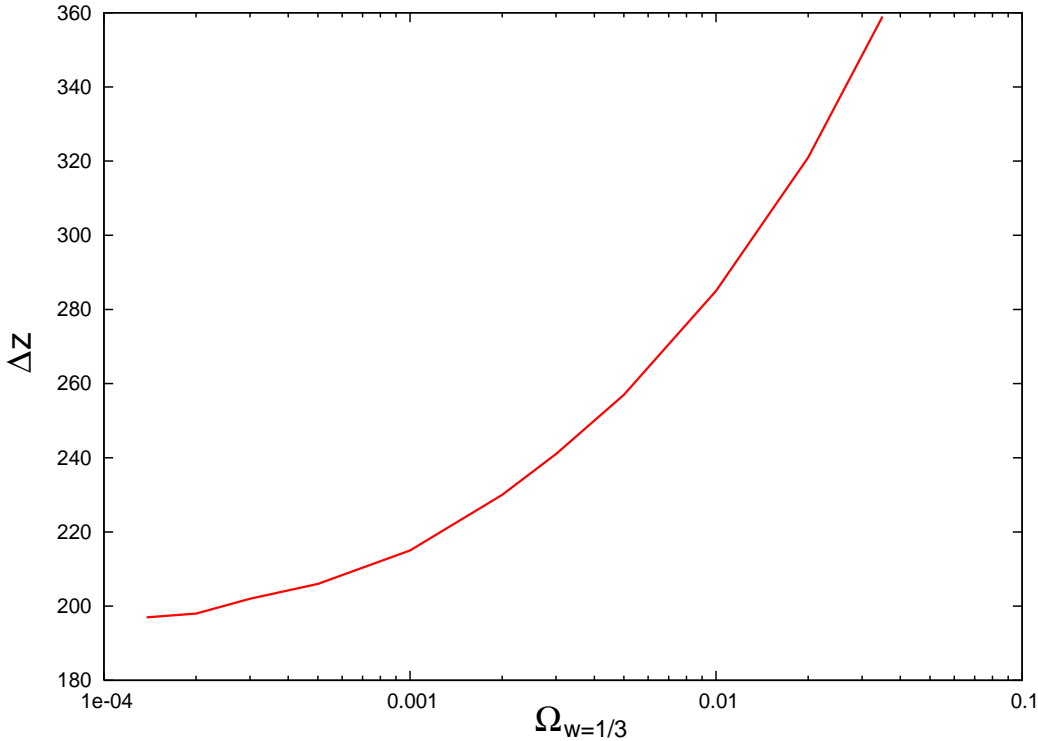


Figure 6. Thickness of the Last Scattering surface as a function of the effective radiation like energy density. The red line runs from the value predicted from the CMB in Λ CDM to the value which best fits the high redshift expansion for the $1/R$ model which best fits the data.

and the recombination coefficient α is described by the expression

$$\alpha = \Sigma_{n,l} \frac{(2l+1)8\pi}{c^2} \left(\frac{kT}{2\pi m_e} \right)^{3/2} \exp \left(\frac{B_n}{kT} \right) \int_{B_n/kT}^{\infty} \frac{\sigma_{nly} y^2 dy}{\exp(y) - 1} \quad (20)$$

Solution of equation (17) gives the ionisation fraction as a function of redshift. Following [32], we approximate α to be $\alpha \propto T^{-0.5}$ and normalise it so that it gives rise to the correct redshift for ionization as observed by WMAP. The thickness of the CMB can then be found by looking at the probability for finding a photon reaching us from a redshift z , $g(z) = e^{-\tau} d\tau/dz$. We then define the thickness as being the full width at half the maximum of this function $g(z)$. In this way we obtain a thickness for the CMB of $\Delta z = 197$ rather close to the WMAP value $\Delta z = 195$.

Figure 6 shows us the thickness of the CMB as a function of the effective radiation density. The greater the expansion of the universe at the last scattering, the more gradual is the era of recombination (gradual with respect to redshift rather than time) and the larger the thickness of the last scattering surface. The redshift of the last scattering surface also changes, but the fractional change in the thickness is much greater. The thickness observed by WMAP is $\Delta z = 195 \pm 2$ [34], however we find that the thickness of the last scattering surface increases to $\Delta z \sim 350$ when the $1/R$ cosmology is studied. So it appears that the best fit to the expansion history data is

incompatible with the thickness of the last scattering surface at some large confidence level ($\sim 77\sigma$).

In summary, the $1/R$ models which fit the supernova and baryon oscillation data can therefore be ruled out because they will lead to a last scattering surface which is too thick.

5. Summary and Conclusions

In this paper we have put cosmological constraints on models where the dark energy component of the universe is explained by theories where gravity is modified by the addition of terms to the Einstein Hilbert Lagrangian which contain inverse powers of the Ricci scalar R .

We find that both $1/R$ and $1/R^2$ models, when forced to fit the supernova data, give rise to solutions at high redshifts where the scale factor $a \propto t^{1/2}$. The universe does not therefore have a matter dominated phase, but rather interpolates between an accelerating phase at low redshifts and a 'radiation-dominated' phase at high redshifts. The expansion at this earlier phase is driven not by radiation which we know the density of by observing the temperature of the CMB. Rather this radiation-like expansion is due to the modified Friedman equations in this class of models.

Despite this, we can still find solutions for the Hubble expansion $H(z)$ that are consistent with the recent supernova results, the baryon acoustic peak and the CMB shift parameter. It is therefore necessary to use other observations to rule these models out. It has been shown elsewhere that perturbations could work against these models [31], here we show a simpler way to rule out such solutions would be to look at the thickness of the last scattering surface.

Acknowledgments

We are very happy to thank Ariel Goobar, Jakob Jonsson, Jakob Nordin and Michel Tytgat for conversations. MF thanks the Perimeter Institute for Theoretical Physics for their hospitality while some of this work was performed.

- [1] P. Astier, *et al.*, A&A, **447**, 31, (2006)
- [2] A. Riess *et al.*, ApJ in press, [astro-ph/0611572]
- [3] G. Miknaitis *et al.*, arXiv:astro-ph/0701043. W. M. Wood-Vasey *et al.*, arXiv:astro-ph/0701041.
- [4] S. Rydbeck, M. Fairbairn and A. Goobar, arXiv:astro-ph/0701495.
- [5] D. N. Spergel *et al.*, arXiv:astro-ph/0603449.
- [6] S. Cole *et al.* [The 2dFGRS Collaboration], Mon. Not. Roy. Astron. Soc. **362** (2005) 505 [arXiv:astro-ph/0501174].
- [7] M. Tegmark *et al.* [SDSS Collaboration], Phys. Rev. D **69** (2004) 103501 [arXiv:astro-ph/0310723].
- [8] D. J. Eisenstein *et al.* [SDSS Collaboration], Astrophys. J. **633** (2005) 560 [arXiv:astro-ph/0501171].
- [9] A. N. Aguirre, Astrophys. J. **512** (1999) L19 [arXiv:astro-ph/9811316].
- [10] C. Csaki, N. Kaloper and J. Terning, Phys. Rev. Lett. **88** (2002) 161302 [arXiv:hep-ph/0111311].

- [11] J. Evslin and M. Fairbairn, *JCAP* **0602** (2006) 011 [arXiv:hep-ph/0507020].
- [12] S. Capozziello, S. Carloni and A. Troisi, arXiv:astro-ph/0303041.
- [13] S. M. Carroll, V. Duvvuri, M. Trodden and M. S. Turner, *Phys. Rev. D* **70** (2004) 043528 [arXiv:astro-ph/0306438].
- [14] T. Chiba, *Phys. Lett. B* **575** (2003) 1 [arXiv:astro-ph/0307338].
- [15] R. Dick, *Gen. Rel. Grav.* **36** (2004) 217 [arXiv:gr-qc/0307052].
- [16] A. D. Dolgov and M. Kawasaki, *Phys. Lett. B* **573** (2003) 1 [arXiv:astro-ph/0307285].
- [17] T. Faulkner, M. Tegmark, E. F. Bunn and Y. Mao, arXiv:astro-ph/0612569.
- [18] J. Khoury and A. Weltman, *Phys. Rev. Lett.* **93** (2004) 171104 [arXiv:astro-ph/0309300].
- [19] E. E. Flanagan, *Phys. Rev. Lett.* **92** (2004) 071101 [arXiv:astro-ph/0308111].
- [20] M. Amarzguioui, O. Elgaroy, D. F. Mota and T. Multamaki, *Astron. Astrophys.* **454** (2006) 707 [arXiv:astro-ph/0510519].
- [21] S. Fay, R. Tavakol and S. Tsujikawa, arXiv:astro-ph/0701479.
- [22] J. Guy, P. Astier, S. Nobili, N. Regnault and R. Pain, arXiv:astro-ph/0506583.
- [23] A. G. Riess, W. H. Press and R. P. Kirshner, *Astrophys. J.* **473** (1996) 88 [arXiv:astro-ph/9604143].
S. Jha, A. G. Riess and R. P. Kirshner, arXiv:astro-ph/0612666.
- [24] M. Fairbairn and A. Goobar, *Phys. Lett. B* **642** (2006) 432 [arXiv:astro-ph/0511029].
- [25] V. Barger, Y. Gao and D. Marfatia, arXiv:astro-ph/0611775.
- [26] Y. Wang and P. Mukherjee, *Astrophys. J.* **650** (2006) 1 [arXiv:astro-ph/0604051].
- [27] K. i. Maeda, *Phys. Rev. D* **39** (1989) 3159.
- [28] L. Amendola, D. Polarski and S. Tsujikawa, arXiv:astro-ph/0603703.
- [29] L. Amendola, R. Gannouji, D. Polarski and S. Tsujikawa, arXiv:gr-qc/0612180.
- [30] B. Chaboyer, P. Demarque, P. J. Kernan and L. M. Krauss, *Astrophys. J.* **494** (1998) 96 [arXiv:astro-ph/9706128].
- [31] R. Bean, D. Bernat, L. Pogosian, A. Silvestri and M. Trodden, arXiv:astro-ph/0611321.
- [32] P. J. E. Peebles, *Astrophys. J.* **153** (1968) 1.
- [33] M. Kaplinghat, R. J. Scherrer and M. S. Turner, *Phys. Rev. D* **60** (1999) 023516 [arXiv:astro-ph/9810133].
- [34] C. L. Bennett *et al.*, *Astrophys. J. Suppl.* **148** (2003) 1 [arXiv:astro-ph/0302207].